$$\frac{\partial C}{\partial t} + U_i \frac{\partial C}{\partial x_i} = \frac{\partial}{\partial x_i}(D_t \frac{\partial C}{\partial x_i}) \quad (7)$$

The turbulent diffusion coefficient D_t in equation (7) is modeled by the relationship eddy-viscosity and the turbulent Schmidt number, $Sc_t = \frac{\nu_t}{D_t}$

In this study, a value of Sc_t = 0.9 has been chosen as in previous studies of pollutant spreading in street canyons.

3 Boundary Conditions

At the inlet, the Dirichlet boundary condition is applied for velocity, turbulent kinetic energy and specific dissipation rate. The inlet velocity profile was prescribed in the power law as in Rafailidis [7]:

$$\frac{U(z)}{U(\delta)} = \left(\frac{z - D}{\delta - D}\right)^{\alpha}$$

The parameters are obtained from the measurement, where: α=0.28, D=0.002m is the displacement height above the ground, $U(\delta)$=5m/s is free-stream velocity, δ=0.5m is the thickness of boundary layer.

The turbulence parameters of k-ω turbulence model is set as follows:

$$k = \frac{3}{2}(UI)^2, \quad \omega = C_{\mu}^{-0.25}\frac{k^{0.5}}{l}$$

where U is mean value of velocity at the inlet; I is the turbulent intensity; C_{μ} = 0.09 is a turbulence model constant; l is the turbulent characteristic length.

No-slip condition was set for velocity at the building walls and road surface. The turbulence parameters such as turbulent kinetic energy and specific dissipation rate were set to wall functions at the wall.

At the symmetry and outlet all variables, such as velocity, pressure and turbulence parameters were set to zero gradient boundary condition.

4 Validations

The numerical simulation has been validated against the experiments of Rafailidis and Schatzmann [3] and Rafailidis [4] with different flat and slanted roof shapes.

4.1 Flat-shaped roof

The modeled street canyon consisted of eight idealized streets. The aspect ratio of the building height H and the width b of the street is 1, whereby H=b=60 mm. There is a steady source C=150 ppm at the bottom center of the fourth street canyon. The geometry is shown in Figure 2 below

Figure 3 shows the streamline of velocity from the numerical results. It shows that the vortices are located in the center of the street canyon. Figure 4 shows a comparison between the observation and numerical results of the vertical velocity

profile at upstream (x/b = - 0.25), center line (x/b = 0) and downstream (x/b = 0.25) of the center line of the fourth street canyon. Figure 5 shows a comparison of the dimensionless concentration *K* (Eq. 8) between the observation and numerical results.

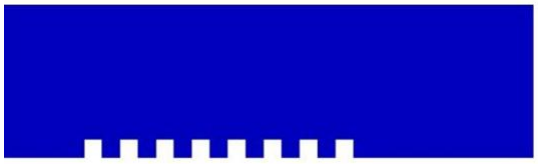

Fig. 2. The geometry of flat-shaped roof

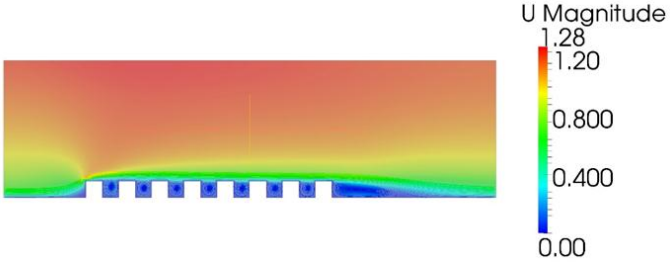

Fig. 3. Streamline of wind flow over flat-shaped roofs

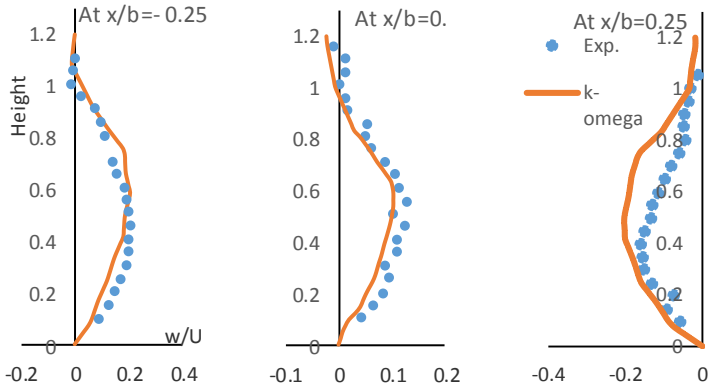

Fig. 4. A comparison between observation and numerical results of vertical velocity profile in the center canyon (windward: x/b=-0.25, center: x/b=0, leeward: x/b=0.25)

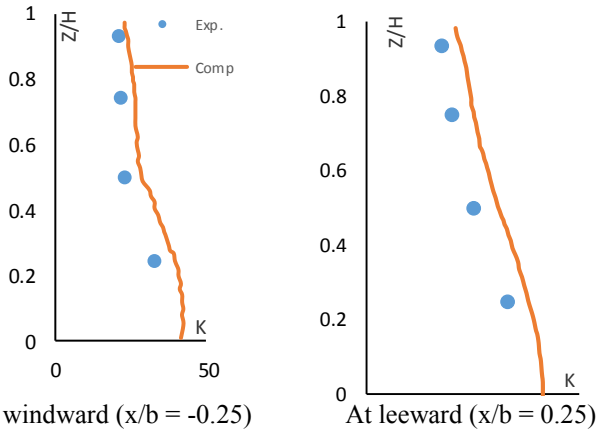

Fig. 5. A comparison of dimensionless concentration K between observation and numerical results in the center canyon

Non-dimensional concentration:

$$K=CUHL/Q \quad (8)$$

Where: C [ppm] is the tracer concentration; U [m/s] is free stream velocity; H [m] is building height; L [m] is length of line source; and Q [m^3/s] is total emission strength.

4.2 Slanted-shaped roof

Similar to the flat roof case, there are 8 buildings with different slanted roof heights with the aspect ratios Z_H/H are of 0.5, 0.33, 0.17 (Z_H is the height of the roof). There is also a steady source L=150 [ppm] at the center of the fourth street canyon. The geometry of the slanted roof shape is shown in Figure 6.

Fig. 6. The geometry of slanted-shaped roof

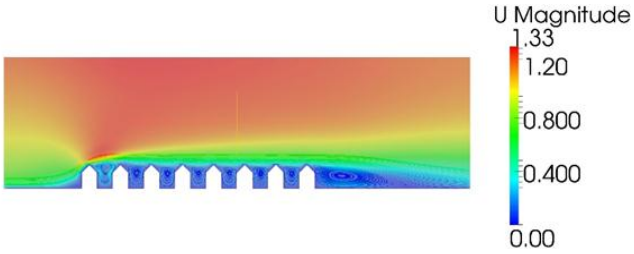

Fig. 7. Streamline of wind flow over slanted-shaped roofs Z_H/H =0.5

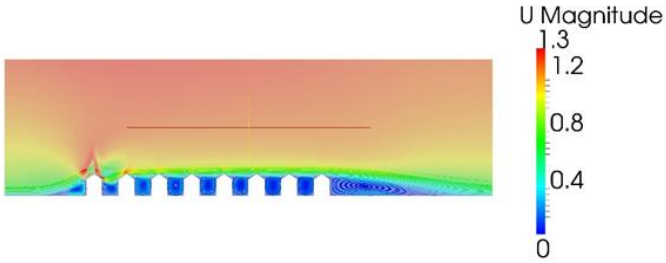

Fig. 8. Streamline of wind flow over slanted-shaped roofs Z_H/H =0.33

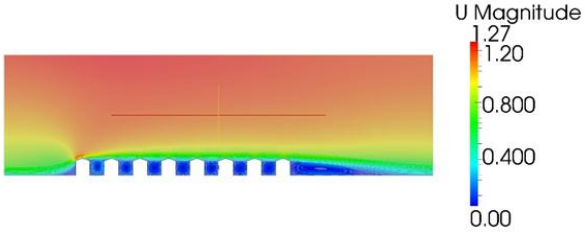

Fig. 9. Streamline of wind flow over slanted-shaped roofs Z_H/H =0.17

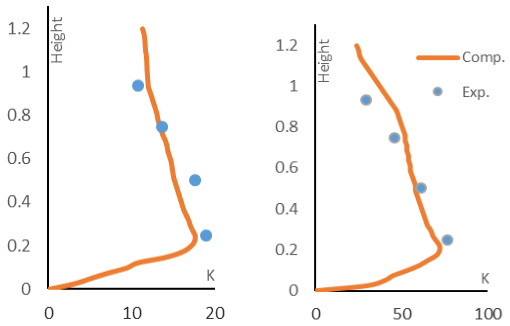

Fig. 10. A comparison of dimensionless concentration K between exp. and comp. at the center canyon

Figures 7, 8 and 9 show the streamline of velocity from the numerical results. It shows that the vortices of wind flow in the street canyon are lifted upward once the slope of the slanted roof is increased, which shows the same results obtained from the simulation by Yassin [8]. The location of the vortex center in the street canyon obtained from our simulation is also very similar to the numerical results of Yassin [8]. Figure 10 shows a comparison of the dimensionless concentration K at upstream (x/b = - 0.25), and downstream (x/b = 0.25) of the center line of the fourth street canyon.

5 Conclusion

As shown above, the numerical model has been verified against benchmarking experiments of Rafailidis and Schatzmann [6], and Rafailidis [7]. The comparisons show a reasonable agreement between the observations and numerical results. It shows the ability of the numerical model, which can be used to calculate the turbulent flows and pollutant transports in urban street canyons. However, before this model can be applied into a real-world applications, a further development and calibrations on different roof's shape and height are of course needed. To capture a better flow patterns and pollutant tracers in the urban street canyons, we plan to implement a higher accurate turbulent calculation, such as Reynolds Stress Model (RSM) or Large Eddy Simulation (LES).

References

1. Baik, J.-J., Kim, J.-J.: A numerical study of flow and pollutant dispersion characteristics in urban street canyons. Journal of Applied Meteorology 38, 1576–1589 (1999).
2. Chan, A.T., Au, W.T.W., So, E.S.P.: Strategic guidelines for street canyon geometry to achieve sustainable street air quality—part II: multiple canopies and canyons. Atmospheric Environment 37 (20), 2761–2772 (2003).
3. Johnson, G.T., Hunter, L.J.: Urban wind flows: wind tunnel and numerical simulations—a preliminary comparison. Environmental Modelling and Software 13, 279–286 (1998).
4. Li, X.-X., Liu, C.-H., Leung, D.Y.C.: Development of a k- ε model for the determination of air exchange rates for street canyons. Atmospheric Environment 39 (38), 7285–7296 (2005).
5. Moonen, P., Gromke, C. and Dorer, V.: Performance assessment of Large Eddy Simulation (LES) for modeling dispersion in urban street canyon with tree planting. Atmospheric Environment 75, 66–76 (2013).
6. Rafailidis, S. and Schatzmann, M.: Concentration Measurements with Different Roof Patterns in Street Canyon with Aspect Ratios B/H=1/2 and B/H=1. Universitaet Hamburg, Meterologisches Institute (1995).
7. Rafailidis, S.: Influence of building area density and roof shape on the wind characteristics above a town. Boundary Layer Meteorology 85, 255–271 (1997).
8. Yassin, M.F.: Impact of height and shape of building roof on air quality in urban street canyons. Atmospheric Environment 43, 5220–5229 (2001).

